Immunostimulatory activity of the aqueous extract from the leaves of *Sambucus racemosa* subsp. *pendula* through TLR4-dependent JNK activation in RAW264.7 cells

HYEOK JIN CHOI[1*], GWANG HUN PARK[2*], JEONG WON CHOI[1], SO JUNG PARK[1], JIN HYUK HWANG[1], SANG HUN LEE[1], HAE-YUN KWON[2], MIN YEONG CHOI[2] and JIN BOO JEONG[1]

[1]Department of Forest Science, Andong National University, Andong, Gyeongsangbuk 36729, Republic of Korea; [2]Forest Medicinal Resources Research Center, National Institute of Forest Science, Yeongju, Gyeongsangbuk 36040, Republic of Korea

Received May 25, 2024; Accepted June 28, 2024

DOI: 10.3892/br.2024.1821

Abstract. *Sambucus racemosa* subsp. *pendula* (SRP) is an endemic plant of Korea, exclusively found on Ulleungdo Island. SRP is widely used as both a traditional medicine and food source. However, there is a lack of research on the pharmacological activities of SRP. Therefore, the present study aimed to explore the potential use of SRP leaves (SRPL) as a natural immunostimulant by analyzing its macrophage activation properties and the underlying mechanisms of action. Among the various extraction conditions, SRPL (AE20-SRPL) extracted with 100% distilled water at 20˚C induced the highest nitric oxide (NO) production in RAW264.7 cells. Thus, the further studies were performed using AE20-SRPL. AE20-SRPL increased the production of immunostimulatory factors such as NO, prostaglandin E2, inducible nitric oxide synthase, cyclooxygenase-2, IL-1β and TNF-α and phagocytosis in a dose-dependent manner in RAW264.7 cells without exhibiting cytotoxicity. Among Toll-like receptor (TLR)2 and TLR4, inhibition of TLR4 significantly reduced AE20-SRPL-mediated increases in the production of immunostimulatory factors and phagocytosis in RAW264.7 cells. Furthermore, in RAW264.7 cells, inhibition of JNK, one of the components of MAPK signaling along with ERK1/2 and p38, attenuated the AE20-SRPL-mediated increases in the production of immunostimulatory factors and phagocytosis. Additionally, AE20-SRPL induced the phosphorylation of JNK and inhibition of TLR4 reduced AE20-SRPL-mediated JNK phosphorylation. These results suggested that AE20-SRPL may enhance the production of immunostimulatory factors and phagocytosis through TLR4-dependent activation of JNK in macrophages. Although the present study is limited to *in vitro* research using a cell model, AE20-SRPL demonstrated potential as a natural material capable of inducing macrophage activation for immune enhancement.

Correspondence to: Professor Jin Boo Jeong, Department of Forest Science, Andong National University, 1375 Gyeongdong-ro, Andong, Gyeongsangbuk 36729, Republic of Korea
E-mail: jjb0403@anu.ac.kr

*Contributed equally

Key words: *Sambucus racemosa* subsp. *pendula*, immunostimulatory activity, macrophages

Introduction

The innate immune system is recognized as the body's first line of defense against pathogens, engaging in the immediate destruction and elimination of pathogens during the initial stages of infection (1). This primary response mechanism is crucial for preventing the establishment and spread of infectious agents (1). Macrophages are recognized as pivotal phagocytes within the innate immune system, playing a crucial role in mediating the initial immune response to pathogens (2). The primary function of macrophages is the phagocytosis of foreign pathogens that invade the human body (3). It is reported that through the process of engulfing these foreign pathogens, macrophages generate a variety of immunostimulatory factors such as nitric oxide (NO), prostaglandin E2 (PGE2), inducible nitric oxide synthase (iNOS), cyclooxygenase-2 (COX-2), IL-1β and TNF-α (4). It is well-documented that various immunostimulatory factors secreted by activated macrophages play a crucial role in the activation of adaptive immune cells, including T cells and B cells (2). Furthermore, macrophages are known to possess a pivotal antigen-presenting capability that is essential for the initiation of the adaptive immune response against invading pathogens (5). Consequently, macrophages are reported to be crucial in both innate and adaptive immune responses (6). Thus, research is currently underway to screen various natural agents capable of activating macrophages, thereby simultaneously enhancing both innate and adaptive immune responses within the body (7-9).

Compared to other species of *Sambucus*, *Sambucus racemosa* subsp. *pendula* (SRP) is distinguished by its smaller berries and unique inflorescence morphology (10). This species is endemic to Korea and is known to be exclusively distributed on Ulleungdo Island (10). The berries of *Sambucus* have

been widely used not only in foods such as jams and juices but also for medicinal purposes (10). However, the Korean Ministry of Food and Drug Safety permits only the leaves and shoots of SRP to be used as food. Nevertheless, studies on the pharmacological effects of leaves and shoots of SRP remain nonexistent. Elderberry, specifically from the *Sambucus* genus (*Sambucus nigra*), has been studied for its immune-boosting properties (11). Thus, the present study investigated the immunostimulatory activity of extracts from the leaves of SRP in RAW264.7 macrophage cells to investigate their potential use as immuno-enhancing products.

Materials and methods

Chemical reagents. 3-(4,5-dimethylthiazol-2-yl)-2,5-diphenyltetrazolium bromide (MTT; cat. no. 475989), PD98059 (cat. no. 513000), SB203580 (cat. no. 58307), SP600125 (cat. no. 55567), TAK-242 (cat. no. 614316), Neutral Red (cat. no. N4638) and Griess reagent (cat. no. G4410) were purchased from MilliporeSigma. C29 (cat. no. 27029) was purchased from Cayman Chemical Company. The primary antibodies such as phosphorylated (p-)JNK (cat. no. 9251), JNK (cat. no. 9258) and β-actin (cat. no. 5125) and the secondary antibody for anti-rabbit IgG, HRP-linked antibody (cat. no. 7074) was purchased from Cell Signaling Technology, Inc.

Sample preparation. Leaves of *Sambucus racemosa* subsp. *pendula* (SRPL; voucher number: FMRC-230501A1-A3) were collected from Ulleungdo Island, Korea in May 2023. SPRL was taxonomically identified by the Forest Medicinal Resources Research Center (Yeongju, South Korea) before being provided for the present study. Ginseng was also provided from the Forest Medicinal Resources Research Center. The freeze-dried SRPL was subjected to an immersion extraction at 20˚C for 24 h using 100% distilled water, 30% ethanol, 50% ethanol and 70% ethanol in a 20-fold volume ratio. Additionally, the freeze-dried SPRL were subjected to immersion extraction with 100% distilled water in a 20-fold volume ratio at 20, 40, 60 and 80˚C for 24 h. The freeze-dried Ginseng (AE20-G) was subjected to immersion extraction with 100% distilled water in a 20-fold volume ratio at 20˚C for 24 h. After 24 h, each extract was centrifuged at 25,200 x g for 10 min at 4˚C and then freeze-dried. The freeze-dried extracts obtained with 100% distilled water were re-dissolved in distilled water, while the freeze-dried ethanol extracts were re-dissolved in dimethyl sulfoxide (DMSO) for use in the experiments.

Cell culture. RAW264.7 murine macrophages (cat. no. TIB-71) were sourced from the American Type Culture Collection. RAW264.7 cells were cultivated in a CO_2 incubator maintained at 37˚C with 5% CO_2 using Dulbecco's Modified Eagle Medium/F-12 (DMEM/F-12; cat. no. SH3023.01; Cytiva) supplemented with 10% fetal bovine serum (FBS; cat. no. 16000-044; Gibco; Thermo Fisher Scientific, Inc.), penicillin (100 units/ml) and streptomycin (100 μg/ml).

Measurement of the viability of RAW264.7 cells. The cytotoxicity of the samples on RAW264.7 cells was evaluated using the MTT assay. RAW264.7 cells ($1x10^5$ cells/well) were cultured in a 96-well plate at 37˚C for 24 h, followed by treatment with the samples (6.25-200 μg/ml) at various concentrations and further incubation at 37˚C for 24 h. The control group (CON) did not undergo any treatment. Subsequently, MTT solution (1 mg/ml) was added to each well and the cells were incubated at 37˚C for an additional 4 h. After this incubation period, the culture medium was removed and the crystallized MTT was dissolved in DMSO. The absorbance was then measured at 570 nm using a UV/visible spectrophotometer (Xma-3000PC; Human Corporation).

Measurement of NO and PGE2 levels in RAW264.7 cells. RAW264.7 cells ($1x10^5$ cells/well) were cultured in a 96-well plate at 37˚C for 24 h, followed by treatment with the samples (6.25-200 μg/ml) at various concentrations and incubation at 37˚C for another 24 h. In addition, RAW264.7 cells were pre-treated with C29 (100 μM), TAK-242 (10 μM), PD98059 (20 μM), SB203580 (20 μM) or SP600125 (20 μM) at 37˚C for 2 h and then co-treated with the sample (50 μg/ml) at 37˚C for 24 h. RAW264.7 cells were cultured in a 96-well plate at 37˚C for 24 h, followed by treatment with AE20-SRPL (50 μg/ml) or AE20-G (50 μg/ml) and incubation at 37˚C for another 24 h. After this incubation period, NO levels were measured using the Griess assay. The cell culture supernatant was mixed with Griess reagent in a 1:1 ratio and allowed to react at room temperature for 15 min. The absorbance was then measured at 540 nm using a UV/Visible spectrophotometer (Xma-3000PC; Human Corporation). PGE2 levels were determined using a Mouse Prostaglandin E2 (PGE2) ELISA Kit (cat. no. MBS266212; MyBioSource, Inc.) according to the protocols provided by the manufacturer.

Measurement of phagocytotic activity in RAW264.7 cells. The effect of the samples on phagocytosis in RAW264.7 cells was evaluated using the Neutral Red uptake assay. RAW264.7 cells ($1x10^5$ cells/well) were cultured in a 96-well plate at 37˚C for 24 h, followed by treatment with the samples (12.5-50 μg/ml) and further incubation at 37˚C for 24 h. In addition, RAW264.7 cells were pre-treated with TAK-242 (10 μM) or SP600125 (20 μM) at 37˚C for 2 h and then co-treated with the sample (50 μg/ml) at 37˚C for 24 h. After this period, the cells were stained with 0.01% Neutral Red solution at 37˚C for 2 h. The stained Neutral Red was then extracted from the cells using a lysis buffer (50% ethanol/1% acetic acid). The absorbance was subsequently measured at 540 nm using a UV/Visible spectrophotometer (Xma-3000PC; Human Corporation).

Reverse transcription-quantitative (RT-q)PCR. RAW264.7 cells ($2x10^6$ cells/well) were cultured in a 6-well plate at 37˚C for 24 h, followed by treatment with the samples (12.5-50 μg/ml) and further incubation at 37˚C for 24 h. In addition, RAW264.7 cells were pre-treated with C29 (100 μM), TAK-242 (10 μM), PD98059 (20 μM), SB203580 (20 μM) or SP600125 (20 μM) at 37˚C for 2 h and then co-treated with the sample (50 μg/ml) at 37˚C for 24 h. Following all treatments, total RNA was isolated from RAW264.7 cells using the RNeasy Mini Kit (cat. no. 74104; Qiagen GmbH) according to the manufacturer's protocol. Subsequently, cDNA was synthesized from 1 μg of total RNA using the Verso cDNA Kit (cat. no. AB1453A; Thermo Fisher Scientific, Inc.) according to the manufacturer's protocol. RT-qPCR was performed

using a Rotor-Gene Q (cat. no. 9001862; Qiagen GmbH) with a QuantiTect SYBR Green PCR kit (cat. no. 204143; Qiagen GmbH) and primers according to the manufacturer's protocol. RT-qPCR cycling conditions were as follows: initial denaturation at 95˚C for 5 min, 30 cycles of denaturation at 95˚C for 15 sec, annealing at 55˚C for 30 sec, and extension at 72˚C for 30 sec to 1 min, followed by a final extension at 72˚C for 10 min, with an optional hold at 4˚C. Data analysis was conducted using Rotor-Gene Q Series software 2.3.5 (Qiagen GmbH). Transcription levels were normalized to those of the GAPDH gene. The formula used to analyze mRNA expression was $2^{-\Delta\Delta Cq}$, where $\Delta\Delta Cq=(Ct_{target}-Ct_{GAPDH})$ sample-$(Ct_{target}-Ct_{GAPDH})$control (12). The sequences of the primers used in the present study were as follows: iNOS mRNA, Forward: 5'-GTTACCATGAGGCTGAAATCC-3' and Reverse: 5'-CCTCTTGTCTTTGACCCAGTAC-3'; COX-2 mRNA, Forward: 5'-CTGGAACATGGACTCACT CAGTTTG-3' and Reverse: 5'-AGGCCTTTGCCACTGCTT GT-3'; IL-1β mRNA, Forward: 5'-GGTACATCAGCACCT CAC-3' and Reverse: 5'-AAACAGTCCAGCCCATAC-3'; TNF-α mRNA, F: 5'-CTCTTCTCATTCCTGCTTG-3' and Reverse: 5'-CTCCACTTGGTGGTTTGT-3'; GAPDH mRNA, Forward: 5'-GGACCTCATGGCCTACATGG-3' and Reverse: 5'-TAGGGCCTCTCTTGCTCAGT-3'.

SDS-PAGE and western blot analysis. RAW264.7 cells ($2x10^6$ cells/well) were cultured in a 6-well plate at 37˚C for 24 h. Then, RAW264.7 cells were treated with the samples (50 μg/ml) at 37˚C for 1, 3, 6, 10, or 24 h. In addition, RAW264.7 cells were pretreated with TAK-242 (10 μg/ml) at 37˚C for 2 h and then co-treated with the sample (50 μg/ml) at 37˚C for 1 h. After washing with phosphate-buffered saline, proteins were extracted from RAW264.7 cells using a radioimmunoprecipitation assay buffer (cat. no. BP-115DG; Boston BioProducts, Inc.). The resulting lysates were centrifuged at 4˚C and 25,200 x g for 30 min. Protein concentrations were quantified using Pierce BCA Protein Assay Kits (cat. no. 23225; Thermo Fisher Scientific, Inc.). The proteins (50 μg/well) were then separated via SDS-PAGE (12% polyacrylamide gel) and subsequently transferred to nitrocellulose membranes (0.45 μm; cat. no. 88018; Thermo Fisher Scientific, Inc.). These membranes underwent a blocking step using 5% nonfat milk for 1 h at ambient temperature, followed by overnight incubation with primary antibodies (dilution 1:1,000) at 4˚C. This was succeeded by a one-hour incubation with secondary antibodies (dilution 1:1,000) at room temperature. After treatment with ECL Select Western Blotting Detection Reagent (cat. no. RPN2232; Cytiva), visualization of the protein bands was accomplished using an LI-COR C-DiGit Blot Scanner (LI-COR Biosciences). The intensity of these protein bands was quantitatively determined using the UN-SCAN-IT gel software version 5.1 (Silk Scientific Inc.).

Statistical analysis. All experiments were repeated at least thrice. Statistical analyses were conducted using GraphPad Prism version 5.0 (Dotmatics) and data are represented as the mean ± standard deviation. All data were analyzed using one-way analysis of variance, followed by Bonferroni's post-hoc test. $P<0.05$ was considered to indicate a statistically significant difference.

Results

AE20-SRPL induces macrophage activation in RAW264.7 cells. To investigate the role of SRPL in inducing macrophage activation, we examined the changes in immunostimulatory factors and phagocytic activity in RAW264.7 cells treated with SRPL. To determine the optimal extraction condition for SRPL, a comparative analysis of SRPL extracted by 100% distilled water (AE-SRPL), 30% ethanol (30EE-SRPL), 50% ethanol (50EE-SRPL), or 70% ethanol (70EE-SRPL) on NO production in RAW264.7 cells was conducted. As shown in Fig. 1A, AE-SRPL significantly induced NO production compared with the control, demonstrating its potential as an immunostimulant, whereas 30EE-SRPL induced only a modest increase and 50EE-SRPL and 70EE-SRPL barely induced NO production. Therefore, to determine whether the extraction temperature of SRPL affected NO production in RAW264.7 cells, NO production in RAW264.7 cells treated with SRPL extracts obtained at 20˚C (AE20-SRPL), 40˚C (AE40-SRPL), 60˚C (AE60-SRPL) and 80˚C (AE80-SRPL) were compared and analyzed. As shown in Fig. 1B, RAW264.7 cells treated with AE20-SRPL and AE40-SRPL exhibited significant increases in NO production. By contrast, AE60-SRPL and AE80-SRPL did not induce any notable enhancement in NO production in these cells. Given that AE20-SRPL induced a higher production of NO than AE40-SRPL, AE20-SRPL was selected for further investigation. As shown in Fig. 2A, AE20-SRPL (6.25-200 μg/ml) elicited a statistically significant, concentration-dependent increase in the production of NO and PGE2 in RAW264.7 cells. To determine whether the AE20-SRPL-mediated increases in NO and PGE2 production were due to elevated expression of iNOS and COX-2, respectively, the mRNA expression changes of iNOS and COX-2 in RAW264.7 cells treated with AE20-SRPL were analyzed using RT-qPCR analysis. As shown in Fig. 2B, AE20-SRPL (12.5-50 μg/ml) significantly enhanced the mRNA expression of iNOS and COX-2. Additionally, AE20-SRPL (12.5 μg/ml ~50 μg/ml) also elevated the mRNA expression of IL-1β and TNF-α in RAW264.7 cells (Fig. 2C). To assess whether AE20-SRPL activates phagocytic functions in macrophages, changes in phagocytic activity in RAW264.7 cells treated with AE20-SRPL were analyzed using the neutral red uptake assay. As shown in Fig. 2D, AE20-SRPL (12.5-50 μg/ml) was found to activate phagocytic functions in RAW264.7 cells in a concentration-dependent manner. Finally, the effect of AE20-SRPL on cell viability in RAW264.7 cells was assessed using MTT assay. The results indicated that AE20-SRPL, across a concentration range from 6.25-200 μg/ml, did not adversely affect the viability of RAW264.7 cells, indicating that AE20-SRPL is non-toxic to macrophages at the tested concentrations (Fig. 2E). Additionally, to ascertain the extent of macrophage activation induced by AE20-SRPL, the NO production in RAW264.7 cells stimulated by AE20-SRPL or the well-known immunostimulant ginseng (AE20-G) were compared. As shown in Fig. 2F, in RAW264.7 cells stimulated with AE20-SRPL, a greater increase in NO production was observed compared with cells stimulated with AE20-G.

AE20-SRPL induces macrophage activation in a Toll-like receptor (TLR)4-dependent manner in RAW264.7 cells. To evaluate the contributions of TLR2 and TLR4 to

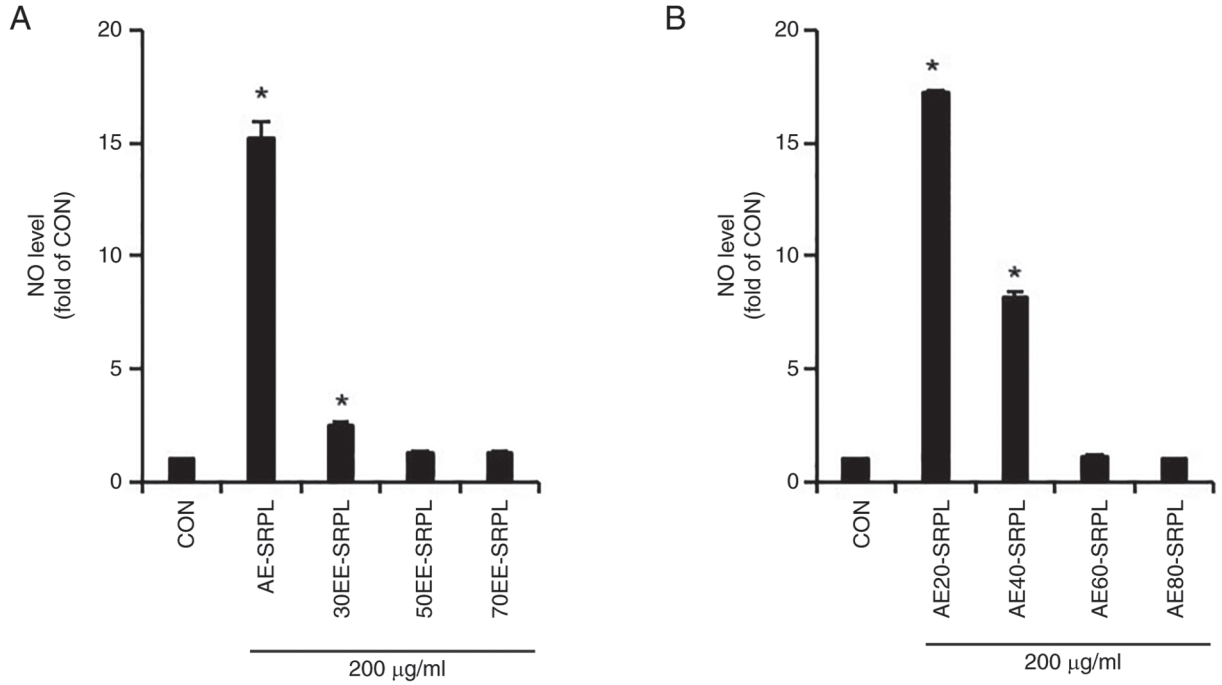

Figure 1. Comparison of NO production induction activity based on extraction conditions of SRPL. (A) AE-SRPL, 30EE-SRPL, 50EE-SRPL or 70EE-SRPL was administered to RAW264.7 cells for 24 h. The level of NO was measured using Griess assay. (B) AE20-SRPL, AE40-SRPL, AE60-SRPL, or AE80-SRPL was administered to RAW264.7 cells for 24 h. The level of NO was measured using Griess assay. *P<0.05 vs. CON. NO, nitric oxide; AE-SRPL, aqueous extracts from SRPL; 30EE-SRPL, 30% ethanol extracts from SRPL; 50EE-SRPL, 50% ethanol extracts from SRPL; 70EE-SRPL, 70% ethanol extracts from SRPL; AE20-SRPL, aqueous extracts from SRPL at 20˚C; AE40-SRPL, aqueous extracts from SRPL at 40˚C; AE60-SRPL, aqueous extracts from SRPL at 60˚C; AE80-SRPL, aqueous extracts from SRPL at 80˚C; CON, control.

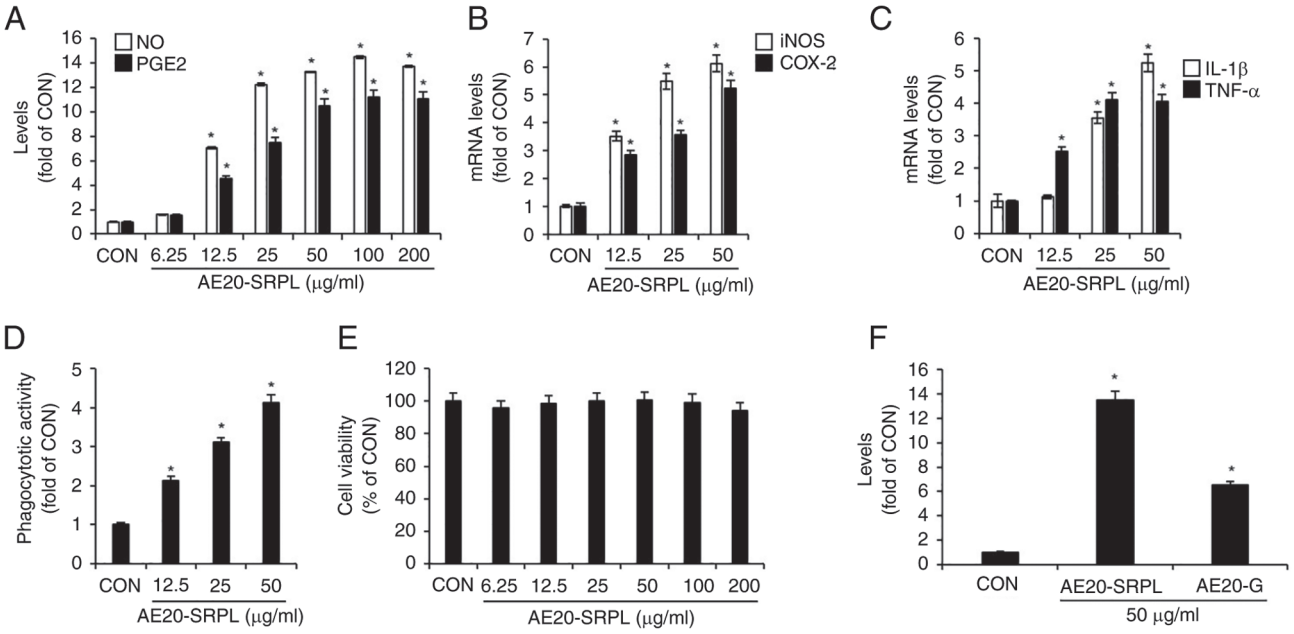

Figure 2. Effect of AE20-SRPL on macrophage activation in RAW264.7 cells. (A) AE20-SRPL was administered to RAW264.7 cells for 24 h. The levels of NO and PGE2 were measured using Griess assay and ELISA kit, respectively. (B and C) AE20-SRPL was administered to RAW264.7 cells for 24 h. The mRNA levels of iNOS and COX-2, IL-1β and TNF-α were measured using reverse transcription-quantitative PCR. (D) AE20-SRPL was administered to RAW264.7 cells for 24 h. Phagocytotic activity was measured using the neutral red uptake method. (E) AE20-SRPL was administered to RAW264.7 cells for 24 h. Cell viability was measured using MTT assay. (F) AE20-SRPL or AE20-G was administered to RAW264.7 cells for 24 h. The NO level was measured using Griess assay. *P<0.05 vs. CON. AE20-SRPL, aqueous extracts from SRPL at 20˚C; AE20-G. aqueous extracts from ginseng at 20˚C; NO, nitric oxide; PGE2, prostaglandin E2; iNOS, inducible nitric oxide synthase; COX-2, cyclooxygenase-2; IL-1β, interleukin-1β; TNF-α, tumor necrosis factor-α; CON, control.

AE20-SRPL-mediated macrophage activation, the present study treated AE20-SRPL to RAW264.7 cells in which TLR2 was inhibited by C29 or TLR4 was inhibited by TAK-242 and then analyzed changes in the production of NO and PGE2.

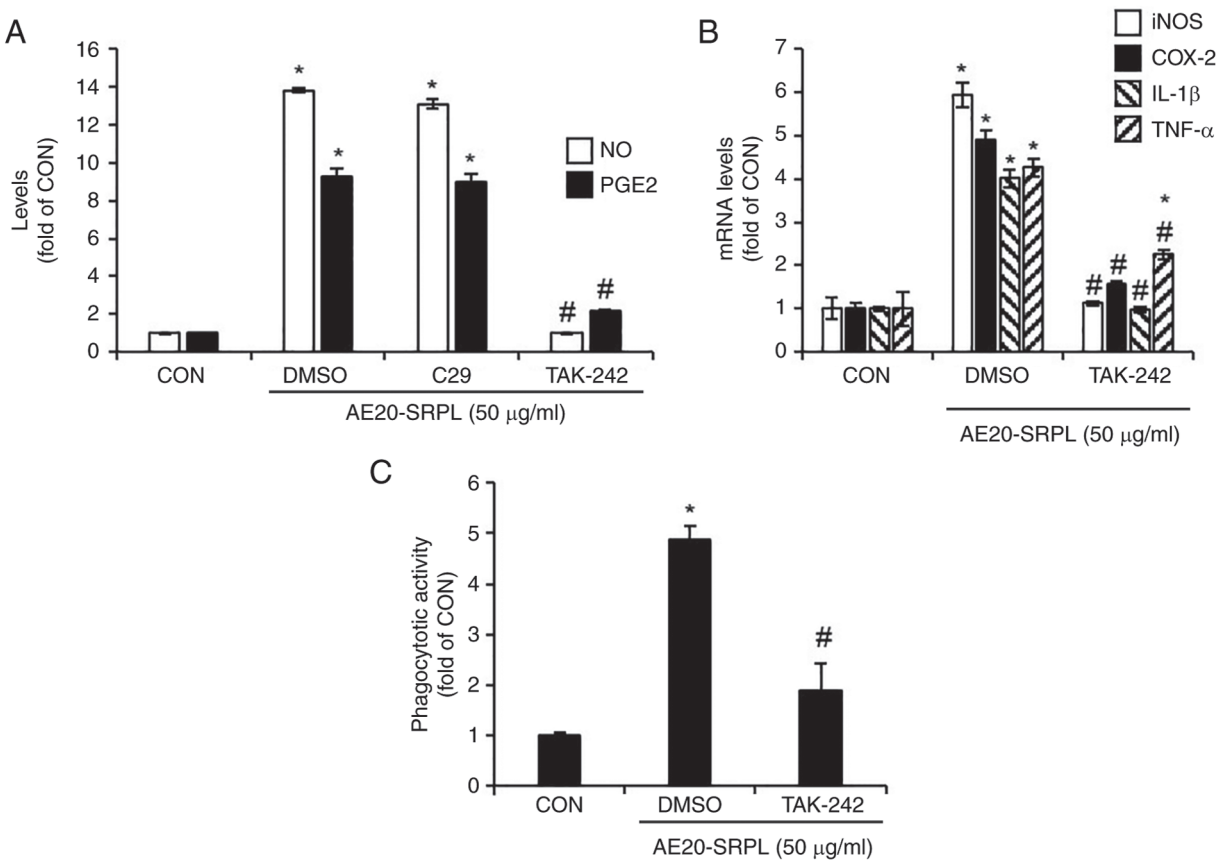

Figure 3. Effect of TLR2 and TLR4 on AE20-SRPL-mediated activation of macrophages in RAW264.7 cells. (A) RAW264.7 cells were pretreated with C29 (TLR2 inhibitor, 100 μM) or TAK-242 (TLR4 inhibitor, 10 μM) for 2 h and then co-treated with AE20-SRPL (50 μg/ml) for 24 h. The levels of NO and PGE2 were measured using Griess assay and ELISA kit, respectively. (B) RAW264.7 cells were pretreated with TAK-242 (TLR4 inhibitor, 10 μM) for 2 h and then co-treated with AE20-SRPL (50 μg/ml) for 24 h. The mRNA levels of iNOS and COX-2, IL-1β and TNF-α were measured using reverse transcription-quantitative PCR. (C) RAW264.7 cells were pretreated with TAK-242 (TLR4 inhibitor, 10 μM) for 2 h and then co-treated with AE20-SRPL (50 μg/ml) for 24 h. Phagocytotic activity was measured using the neutral red uptake method. *P<0.05 vs. CON. #P<0.05 vs. DMSO. TLR, Toll-like receptor; AE20-SRPL, aqueous extracts from SRPL at 20˚C; NO, nitric oxide; PGE2, prostaglandin E2; iNOS, inducible nitric oxide synthase; COX-2, cyclooxygenase-2; IL-1β, interleukin-1β; TNF-α, tumor necrosis factor-α; CON, control.

The results demonstrated that inhibition of TLR2 had no significant effect on the AE20-SRPL-mediated increase in NO and PGE2 production (Fig. 3A). By contrast, inhibition of TLR4 markedly reduced these increases (Fig. 3A). Thus, the effect of TLR4 inhibition on AE20-SRPL-mediated effects were investigated, specifically examining the expression of iNOS, COX-2, IL-1β and TNF-α, as well as the activation of phagocytic functions in macrophages. The results indicated that TLR4 inhibition by TAK-242 significantly reduced the AE20-SRPL-mediated expression of iNOS, COX-2, IL-1β and TNF-α (Fig. 3B). Furthermore, this inhibition also suppressed the activation of phagocytic functions in macrophages induced by AE20-SRPL (Fig. 3C).

AE20-SRPL induces macrophage activation in a JNK-dependent manner in RAW264.7 cells. To evaluate the contributions of MAPKs ERK1/2, p38 and JNK signaling to AE20-SRPL-mediated macrophage activation, AE20-SRPL to RAW264.7 cells were treated in the absence or presence of PD98059 (ERK1/2 inhibitor), SB203580 (p38 inhibitor) or SP600125 (JNK inhibitor) and then changes in the production of NO and PGE2 analyzed. As shown in Fig. 4A, inhibitions of ERK1/2 by PD98059 and p38 by SB203580 had no significant effect on the AE20-SRPL-mediated increase in NO and PGE2 production. However, the inhibition of JNK by SP600125 blocked these increases. Thus, it was investigated whether the inhibition of JNK signaling pathways would also affect the AE20-SRPL-mediated expression of iNOS, COX-2, IL-1β and TNF-α. The results demonstrated that in RAW264.7 cells where JNK was inhibited, there was a notable reduction in the expressions of iNOS, COX-2, IL-1β and TNF-α by AE20-SRPL (Fig. 4B). Furthermore, a decrease in AE20-SRPL-mediated activation of phagocytic functions in RAW264.7 cells where JNK was individually inhibited was observed (Fig. 4C). To investigate whether AE20-SRPL activates JNK, the phosphorylation of JNK in RAW264.7 cells treated with AE20-SRPL at various time points was analyzed. As shown in Fig. 4D, the results demonstrated an enhancement in the phosphorylation of both JNK in RAW264.7 cells following AE20-SRPL treatment. Furthermore, it was explored whether TLR4 influences the AE20-SRPL-mediated phosphorylation of JNK. In the absence of TAK-242, AE20-SRPL significantly induced the phosphorylation of JNK (Fig. 4E). However, inhibition of TLR4 by TAK-242 resulted in a marked reduction in AE20-SRPL-mediated phosphorylation of JNK (Fig. 4E).

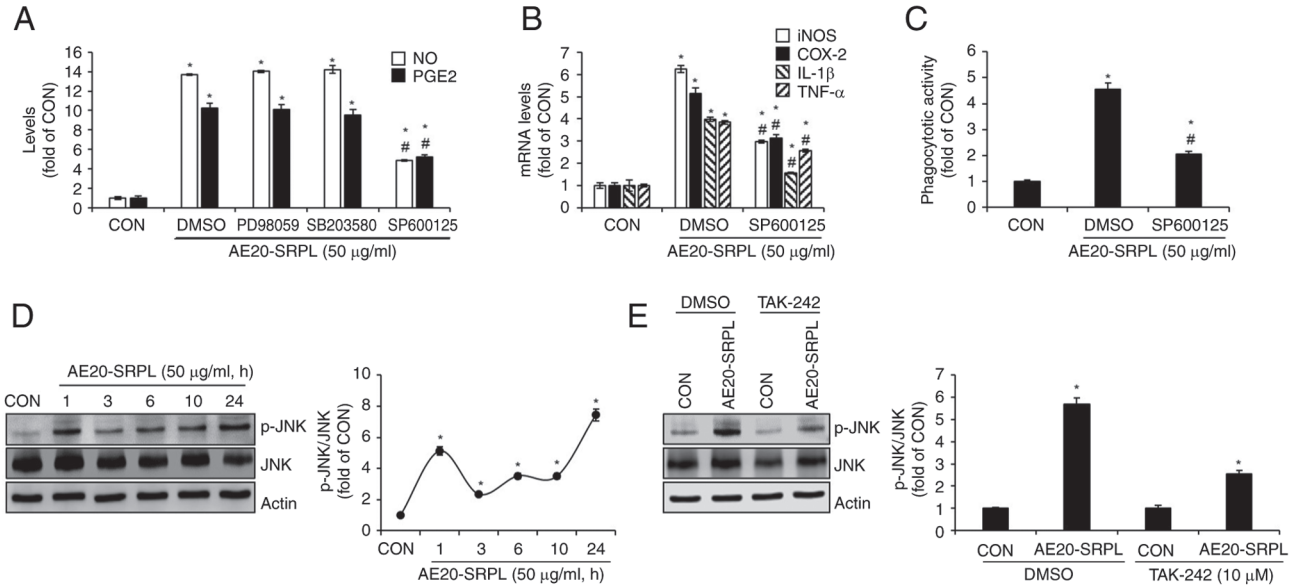

Figure 4. Effect of MAPK signaling pathways on AE20-SRPL-mediated activation of macrophages in RAW264.7 cells. (A) RAW264.7 cells were pretreated with PD98059 (ERK1/2 inhibitor; 20 μM), SB203580 (p38 inhibitor; 20 μM) or SP600125 (JNK inhibitor; 20 μM) and then co-treated with AE20-SRPL (50 μg/ml) for 24 h. The levels of NO and PGE2 were measured using Griess assay and ELISA kit, respectively. (B) RAW264.7 cells were pretreated with SP600125 (JNK inhibitor; 20 μM) and then co-treated with AE20-SRPL (50 μg/ml) for 24 h. The mRNA levels of iNOS and COX-2, IL-1β and TNF-α were measured using reverse transcription-quantitative PCR. (C) RAW264.7 cells were pretreated with SP600125 (JNK inhibitor; 20 μM) and then co-treated with AE20-SRPL (50 μg/ml) for 24 h. Phagocytotic activity was measured using the neutral red uptake method. (D) RAW264.7 cells were treated with AE20-SRPL (50 μg/ml) for the indicated time-points. p-JNK, JNK and Actin were measured using western blot analysis. (E) RAW264.7 cells were pretreated with TAK-242 (TLR4 inhibitor, 10 μM) for 2 h and then co-treated with AE20-SRPL (50 μg/ml) for 1 h. p-JNK, JNK and Actin were measured using western blot analysis. *P<0.05 vs. CON. $^{\#}$P<0.05 vs. DMSO. AE20-SRPL, aqueous extracts from SRPL at 20˚C; NO, nitric oxide; PGE2, prostaglandin E2; iNOS, inducible nitric oxide synthase; COX-2, cyclooxygenase-2; IL-1β, interleukin-1β; TNF-α, tumor necrosis factor-α; CON, control; p-, phosphorylated; JNK, c-Jun N-terminal kinase.

Discussion

On invasion by foreign pathogens, activated macrophages are known to phagocytize these invaders while concurrently secreting a diverse array of immunostimulatory factors such as NO, PGE2, iNOS, COX-2, IL-1β and TNF-α (4). It has been reported that NO produced by iNOS directly eliminates invading pathogens such as microbes and viruses (13). Furthermore, NO is known to exert a positive influence on the adaptive immune system by promoting the differentiation and activation of T cells (14). PGE2 synthesized by COX-2 is also known to play a pivotal role in the human immune system, influencing both innate and adaptive immune responses, as well as providing critical host defenses against viral, fungal and bacterial pathogens (15). IL-1β contributes to the activation of macrophage phagocytic activity against invading pathogens (16). In addition, IL-1β has been reported to play a pivotal role as an activator of humoral immune responses by contributing to T-cell-dependent antibody production (17). TNF-α is recognized as a key regulatory factor within the immune system, playing a vital role in the immune response against various pathogens (18). TNF-α is integral to both the innate and adaptive immune systems, with a particularly crucial function in modulating T-cell activity within the adaptive immune response (18). These existing reports reflect that these immunostimulatory factors are pivotal in modulating the efficacy and coordination of immune responses, highlighting their integral roles in the maintenance and enhancement of immunological functions. In immune responses, the most critical function of macrophages is known to be their phagocytic activity against pathogens, which initiates the innate immune response and, in turn, orchestrates the adaptive immune response (19). The present study confirmed that AE20-SRPL effectively enhanced the production of immunostimulatory factors such as NO, PGE2, iNOS, COX-2, IL-1β and TNF-α and activated phagocytosis in RAW264.7 cells. Additionally, it was verified that AE20-SRPL did not exhibit cytotoxic effects on RAW264.7 cells. These findings suggested the potential of AE20-SRPL as a natural material that can safely enhance immune function without adverse effects.

For macrophages to produce immunostimulatory factors through phagocytic activity, they must first recognize and become activated by foreign pathogens via pattern recognition receptors (PRRs) (20). This critical recognition step facilitates the activation of macrophages, enabling them to initiate the immune response by engulfing pathogens and subsequently secreting a cascade of immune mediators (20). Among PRRs, Toll-like receptors (TLRs) are known to recognize a broad range of organisms, including bacteria, fungi, protozoa and viruses (20). TLRs known as critical sensors for recognizing foreign pathogens not only play an essential role in the innate immune system but also serve as a vital bridge connecting innate and adaptive immunity (20). Among the TLRs, TLR2 and TLR4 have been reported to play crucial roles in recognizing foreign pathogens and triggering the production of various immunostimulatory factors necessary for antigen presentation (21,22). In the present study, it was observed that in RAW264.7 cells, the

inhibition of C29 had no effect on the production of NO and PGE2 mediated by AE20-SRPL, whereas inhibition of TLR4 significantly reduced the generation of NO and PGE2 mediated by AE20-SRPL. Furthermore, inhibition of TLR4 also decreased the expression of iNOS, COX-2, IL-1β and TNF-α induced by AE20-SRPL and suppressed the activation of phagocytic activity mediated by AE20-SRPL. These results suggested that TLR4 may play a crucial role not only in the direct signaling mechanisms that govern the production of immunostimulatory factors by AE20-SRPL but also in AE20-SRPL-mediated facilitation of the phagocytic capabilities of macrophages, which are essential for the effective clearance of pathogens.

The MAPK pathways comprising ERK1/2, p38 and JNK are known to be intricately linked to the activation of macrophages (23). Thus, the present study investigated which specific signaling pathway among ERK1/2, p38 and JNK was utilized for AE20-SRPL-mediated macrophage activation. The present study confirmed that the inhibition of JNK among the ERK1/2, p38 and JNK signaling pathways reduces the production of immunostimulatory factors and the activation of phagocytosis by AE20-SRPL. Furthermore, AE20-SRPL activates JNK. The data suggested that the JNK pathway is particularly critical in AE20-SRPL-mediated macrophage activation. The immune response of macrophages to foreign pathogens through the activation of JNK has been reported to be dependent on TLR4 (24). Several natural agents have been reported to activate macrophages through TLR4-dependent JNK activation (25,26). Thus, whether TLR4 is involved in the AE20-SRPL-mediated activation of JNK was analyzed. The results demonstrated that inhibition of TLR4 reduces AE20-SRPL-mediated activation of JNK. These findings indicated that the activation of JNK by AE20-SRPL may be TLR4-dependent.

Based on the results of the present study, it can be concluded that AE20-SRPL activates phagocytosis and enhances the production of immunostimulatory factors through TLR4-dependent activation of JNK in macrophages. The present study was valuable as it identified a novel agent capable of inducing macrophage activation for immunoenhancement and elucidates the potential mechanism of action of this agent. However, the present study has three limitations that necessitate further research for the development of the immunostimulatory agent using AE20-SRPL. First, since the present study uses an *in vitro* approach with macrophages, it is imperative to conduct validation studies *in vivo* to ascertain whether AE20-SRPL exhibits immunostimulatory activity in a cyclophosphamide-induced immunosuppression C57BL/6 mice model. The second point is that the present study focused exclusively on the activation of macrophages, which are a critical component of the innate immune system. However, to establish robust evidence for the immuno-enhancing activity of AE20-SRPL, it is necessary to investigate whether AE20-SRPL also affects other types of immune cells. Last, the present study did not conduct a detailed analysis of the specific components of AE20-SRPL related to its immunostimulatory activity. Therefore, it is necessary to perform component analysis studies to identify which constituents of AE20-SRPL are responsible for its immunostimulatory effects.

Acknowledgements

Not applicable.

Funding

The present study was supported by a grant from the National Institute of Forest Science in 2024 (project no. FP0802-2023-01-2024) and the R&D Program for Forest Science Technology (grant no. RS-2024-00405196) provided by the Korea Forest Service (Korea Forestry Promotion Institute, Seoul, Korea).

Availability of data and materials

The data generated in the present study may be requested from the corresponding author.

Authors' contributions

HJC, GHP, JWC, SJP, JHH, SHL, HYK and MYC performed cell-based experiments and analyzed the data. HJC and GHP wrote the manuscript. JBJ designed the experiments and wrote and edited the manuscript. HJC, GHP, JWC, SJP, JHH, SHL, HYK, MYC and JBJ confirm the authenticity of all the raw data. All the authors have read and approved the final version of the manuscript.

Ethics approval and consent to participate

Not applicable.

Patient consent for publication

Not applicable.

Competing interests

The authors declare that they have no competing interests.

References

1. Hirayama D, Iida T and Nakase H: The phagocytic function of macrophage-enforcing innate immunity and tissue homeostasis. Int J Mol Sci 19: 92, 2018.
2. Duque GA and Descoteaux A: Macrophage cytokines: Involvement in immunity and infectious diseases. Front Immunol 5: 491, 2014.
3. Sieweke MH and Allen JR: Beyond stem cells: self-renewal of differentiated macrophages. Science 342: 1242974, 2013.
4. Hume DA: The mononuclear phagocyte system. Curr Opin Immunol 18: 49-53, 2006.
5. Muntjewerff EM, Meesters LD and van den Bogaart G: Antigen cross-presentation by macrophages. Front Immunol 11: 1276, 2020.
6. Gordon S and Mantovani A: Diversity and plasticity of mononuclear phagocytes. Eur J Immunol 41: 2470-2472, 2011.
7. Shin MS, Hwang SH, Yoon TJ, Kim SH and Shin KS: Polysaccharides from ginseng leaves inhibit tumor metastasis via macrophage and NK cell activation. Int J Biol Macromol 103: 1327-1333, 2017.
8. Tabarsa M, Jafari A, You S and Cao R: Immunostimulatory effects of a polysaccharide from Pimpinella anisum seeds on RAW264.7 and NK-92 cells. Int J Biol Macromol 213: 546-554, 2022.
9. Zhang A, Yang X, Li Q, Yang Y, Zhao G, Wang B and Wu D: Immunostimulatory activity of water-extractable polysaccharides from Cistanche deserticola as a plant adjuvant in vitro and in vivo. PLoS One 13: e0191356, 2018.

10. Lim HI: Seed dormancy and germination characteristics of endemic elder species (Sambucus racemose subsp. pendula) and common elder species (S. williamsii) in Korea. J For Environ Sci 38: 284-289, 2022.
11. Mocanu ML and Amariei S: Elderberries-A source of bioactive compounds with antiviral action. Plants (Basel) 11: 740, 2022.
12. Livak KJ and Schmittgen TD: Analysis of relative gene expression data using real-time quantitative PCR and the 2(-Delta Delta C(T)) method. Methods 25: 402-408, 2001.
13. Bogdan C: Nitric oxide synthase in innate and adaptive immunity: An update. Trends Immunol 36: 161-178, 2015.
14. García-Ortiz A and Serrador JM: Nitric oxide signaling in T cell-mediated immunity. Trends Mol Med 24: 412-427, 2018.
15. Martínez-Colón GJ and Moore BB: Prostaglandin E_2 as a regulator of immunity to pathogens. Pharmacol Ther 185: 135-146, 2018.
16. Netea MG, Simon A, van de Veerdonk F, Kullberg BJ, van der Meer JWM and Joosten LAB: IL-1β processing in host defense: Beyond the inflammasomes. PLoS Pathog 6: e1000661, 2010
17. Nakae S, Asano M, Horai R and Iwakura Y: Interleukin-1beta, but not interleukin-1α, is required for T-cell-dependent antibody production. Immunology 104: 402-409, 2001.
18. Vielhauer V and Mayadas TN: Functions of TNF and its receptors in renal disease: Distinct roles in inflammatory tissue injury and immune regulation. Semin Nephrol 27: 286-308, 2007.
19. Aderem A and Underhill DM: Mechanisms of phagocytosis in macrophages. Ann Rev Immunol 17: 593-623, 1999.
20. Zhou L, Cao X, Fang J, Li Y and Fan M: Macrophages polarization is mediated by the combination of PRR ligands and distinct inflammatory cytokines. Int J Clin Exp Pathol 8: 10964-10974, 2015.
21. Beutler B, Jiang Z, Georgel P, Crozat K, Croker B, Rutschmann S, Du X and Hoebe K: Genetic analysis of host resistance: Toll-like receptor signaling and immunity at large. Ann Rev Immunol 24: 353-389, 2006.
22. Takeda K and Akira S: Toll-like receptors in innate immunity. Int Immunol 17: 1-4, 2005.
23. Ren D, Lin D, Alim A, Zheng Q and Yang X: Chemical characterization of a novel polysaccharide ASKP-1 from Artemisia sphaerocephala Krasch seed and its macrophage activation via MAPK, PI3k/Akt and NF-κB signaling pathways in RAW264.7 cells. Food Funct 8: 1299-1312, 2017.
24. Swanson L, Katkar GD, Tam J, Pranadinata RF, Chareddy Y, Coates J, Anandachar MS, Castillo V, Olson J, Nizet V, *et al*: TLR4 signaling and macrophage inflammatory responses are dampened by GIV/Girdin. Proc Natl Acad Sci USA 117: 26895-26906, 2020.
25. Um Y, Eo HJ, Kim HJ, Kim K, Jeon KS and Jeong JB: Wild simulated ginseng activates mouse macrophage, RAW264.7 cells through TRL2/4-dependent activation of MAPK, NF-κB and PI3K/AKT pathways. J Ethnopharmacol 263: 113218, 2020.
26. Xie XD, Tang M, Yi SL, He Y, Chen SY, Zhao Y, Chen Q, Cao MX, Yu ML, Wei YY, *et al*: Polysaccharide of Asparagus cochinchinensis (Lour.) Merr regulates macrophage immune response and epigenetic memory through TLR4-JNK/p38/ERK signaling pathway and histone modification. Phytomedicine 124: 155294, 2024.